Service Life Prediction Under Combined Cyclic and Steady State Tearing.

R.J. Windslow & J.J.C. Busfield

Soft Matter Research Group, Queen Mary University of London, United Kingdom

Materials Research Institute, Queen Mary University of London, United Kingdom

ABSTRACT: In this paper a novel approach for modelling failure under a combination of cyclic and static loading is presented. The cyclic fatigue and steady state tearing performance of two non-strain crystallising elastomers, NBR and EPDM, are initially characterised. A simplified component was then tested to failure using a combined cyclic/steady-state loading regime and its service life is compared against predictions from the developed analytical model.

1 INTRODUCTION

1.1 *Problem Background*

For non-strain crystallising elastomers crack growth can either occur during cyclical loading conditions or under steady state strained conditions providing a threshold tearing energy has been exceeded, Sakulkaew *et al.,* (2011). Most conventional applications fail either under cyclic crack growth or as a result of steady state crack growth and hence the service life can simply be predicted by applying the relevant fracture principal to either one or other of these conditions. Nevertheless, there are some engineering applications, in which the cracks grow through a combination of cyclic and steady state tear conditions. This is much more complicated to model due to the inter-dependence between these two fracture phenomena, which prevents direct integration.

1.2 *Fracture and Fatigue in Elastomers*

As first demonstrated by Rivlin and Thomas (1953), fracture within elastomers is an energy based phenomena. They extended Griffith's (1921) fracture criterion to polymers such as elastomers by taking into consideration the additional energy dissipation effects. They proposed using the tearing energy, *T*. They quantified this as the strain energy, *U*, released as the fracture surface grew by area, *a*:

$$T = \left(\frac{\mathrm{d}U}{\mathrm{d}a}\right)_l \tag{1}$$

As demonstrated by Kadir and Thomas (1981), cracks grow at different rates, depending on the energy at the crack tip. This allows characteristic tear profiles to be built, with typical schematics for this data being shown, Figure 1.
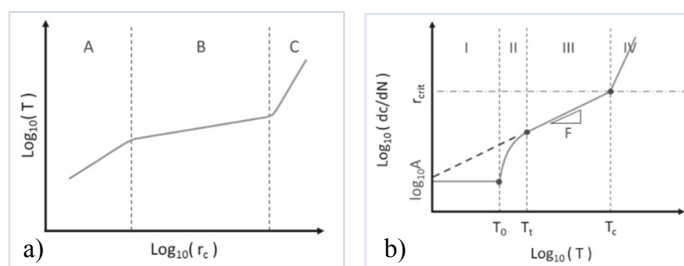

Figure 1: a) Static and b) Cyclic, tear profiles.

When plotted on a logarithmic scale typical static tear profiles split into three linear regions, characteristic with how the crack grows over that range of tear rates, Fukahori *et al*., (2013). Each of the three regions follow a power law relationship. This relates the change in crack length, *c*, with time, *t*, to the tearing energy, *T*, through two material constants, *B* and *β*:

$$\frac{\mathrm{d}c}{\mathrm{d}t} = B(T)^{\beta} \tag{2}$$

Similarly, cyclic fatigue profiles for elastomers break down into four regions when plotted using logarithmic scales, Figure 1b. Most engineering cyclic fatigue problems lie within Region III. Similar to the steady tearing data the data in this region for the rate at which the crack length, *c*, changes with cycle number, *N*, can be also be represented using a power law relationship between the tearing energy, *T*, and two material constants, *A* and *F*:

$$\frac{dc}{dN} = A(T)^F \qquad (3)$$

If one has a purely static or cyclic problem it is relatively simple to integrate the above equations to determine either the time or the number of cycles to failure. By finding the tearing energy as a function of crack length one can simply integrate the function to determine the time or number of cycles to failure.

$$N_f = \int_0^{N_f} dN = \int_{c_0}^{c_f} \frac{dc}{A[T = f(c)]^F} \qquad (4)$$

2 MATHEMATICAL MODEL

2.1 Complex Fatigue System

Some components exhibit a more complex fatigue profile, such as actuated seals. In this case, there are both cyclic and static aspects to the crack growth. During a sealing cycle the seal is deformed into contact with a counter surface before it is then held for a period.

Previously Busfield et al., (2002) have demonstrated that crack growth per cycle can be split into the cyclic, loading phase, and a time dependent, hold phase, Eqn. 5. To differentiate between crack length after a single complete sealing cycle versus during the separate contributions capitals have been used for the full cycle.

$$\frac{dC}{dN} = \left(\frac{dc}{dN}\right)_{Cycle} + \left(\frac{dc}{dN}\right)_{Time} \qquad (5)$$

In service these seals generally only undergo 500-1000 cycles, nevertheless the hold period can last up to 8hrs. Although the number of sealing cycles is relatively low it is impractical to physically replicate this loading regime. This means mathematical models and F.E.A. are the only viable option for predicting and/or determining the component's lifetime.
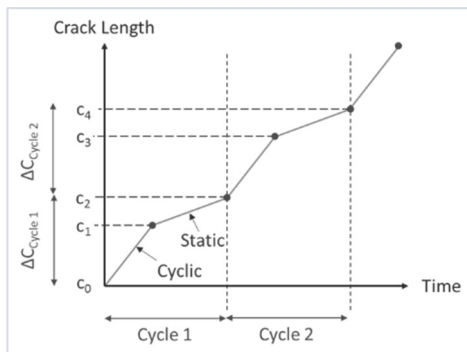

Figure 2: Complex crack growth due to mixed fatigue.

By attempting to directly integrate Eqn. 5 to determine the number of cycles to failure the following equation is achieved, where c_o is the initial crack length and c_f is the crack length at failure.

$$N_f = \sum_{c_i=C_0}^{c_f-2} \left[\int_{c_i}^{c_{i+1}} \frac{dc}{A(T)^F} + \int_{c_{i+1}}^{c_{i+2}} \frac{dc}{B(T)^\beta} \right] \qquad (6)$$

This is nigh on impossible to solve due to the interdependence between the two contributions, Figure 2. A different approach is therefore required.

2.2 Proposed Approach

The authors propose using an Explicit Euler scheme to model the problem. Taking Cycle 1, the cyclic crack growth contribution can be expressed as:

$$\left(\frac{dc}{dN}\right)_{Cycle} = \frac{c_1 - c_0}{\Delta N} = A[T_{Cycle}]^F \qquad (7)$$

Where c_0 is the initial crack length, c_1 is the crack length at the end of the loading stage, ΔN is the change in cycle number, which of cause for this case $\Delta N = 1$, A and F are material constants determined from the material fatigue profile, and T_{Cycle} is the peak tearing energy during loading. It is also a function of crack length:

$$T_{Cycle} = f(c_0) \qquad (8)$$

T_{Cycle} as a function of crack length can simply be found by carrying out an iterative modelling scheme in F.E.A. As the initial crack length, c_0, should be known the only unknown in the expression is the crack length at the transition between the loading and holding stage, c_1, see Figure 2. Eqn. 7 can be adapted to find this unknown.

$$c_1 = \left(A[T_{Cycle}]^F\right) + c_0 \qquad (9)$$

Similarly, the crack growth during the hold stage can be expressed as:

$$\left(\frac{dc}{dN}\right)_{Time} = \frac{c_2 - c_1}{\Delta t} = B[T_{Time}]^\beta \qquad (10)$$

Where c_2 is the crack length at the end of the hold stage, hence the crack length after the first sealing cycle, $c_2 = C_1$. Δt is the time of the hold period, B and β are the material constants from the static tear profile, and T_{Time} is the tearing energy during the hold stage. The only unknown in this expression is c_2 but it can be determined by rearranging the previous equations as before:

$$c_2 = \left(\Delta t * B[T_{Time}]^\beta\right) + c_1 \qquad (11)$$

Combining Eqn. 9 with Eqn. 11 forms a single expression for the crack length at the end of the sealing cycle, C_i, in terms of the initial crack length and the crack growth during the loading and hold stages:

$$C_1 = \left(\Delta t \cdot B[T_{Time}]^\beta\right) + \left(A[T_{Cycle}]^F\right) + c_0 \qquad (12)$$

Iterating to the next step the expression for the crack length at cycle 2, C_2, would be:

$$C_2 = \left(\Delta t \cdot B[T_{Time}]^\beta\right) + \left(A[T_{Cycle}]^F\right) + C_1 \qquad (13)$$

This scheme could be advanced iteratively and hence presents a viable option for modelling fatigue in these complex fatigue problems. However, a difficulty arises as T_{Time} is a function of both crack length, c_1, and time, t, due to viscoelastic relaxation:

$$T_{Time} = f(c_1, t) \qquad (14)$$

In essence, during the hold stage the tearing energy is gradually decaying with time causing the rate of crack growth to decrease.

3 MATERIAL CHARACTERISATION

To better understand this problem two elastomers were characterised before undergoing mixed mode fatigue tests, allowing the mathematical model to be compared against real test data. these tests were undertaken using the pure shear crack growth (also known as the planar tension crack growth) test piece geometry. By using this planar geometry, the tearing energies dependence on crack length was removed, Eqn. 15. This meant the cyclic crack growth should be constant and the static crack growth would only depend on time due to relaxation effects. The characterisation tests were therefore also carried out using this planar crack growth test piece geometry.

3.1 Material Selection

The elastomers used in this study were an NBR and an EPDM typically used for sealing applications. Both elastomers were provided as uncured masterbatch by Clwyd Compounders.

3.2 Cyclic Crack Growth

The cyclic crack growth was characterised on an INSTRON 8801 servo-hydraulic test machine using the planar crack growth test piece geometry. Samples were cut into rectangular strips of 175mm x 45mm x 2mm, before being installed between the clamps.

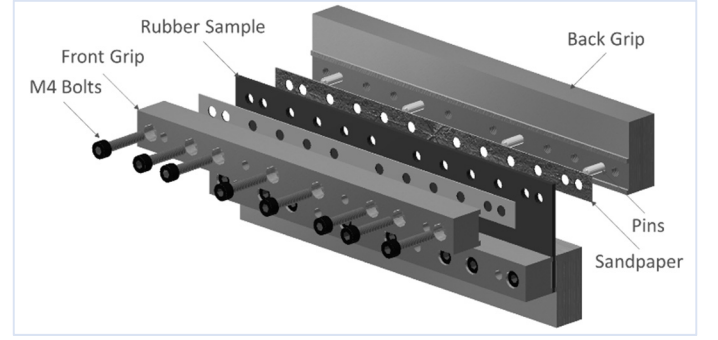Once installed this left a test region of 175mm x 15mm x 2mm.

Figure 3: Exploded drawing of the planar test set-up.

A 30mm flaw was cut into the sample such that the crack tip was a suitably distance from the free edge zones. For the planar crack growth test geometry, the tearing energy is given by:

$$T = wh \qquad (15)$$

Where the tearing energy, T, is the product of the sample's unstrained height, h, and the strain energy density, w, in the pure shear test region. Nevertheless due to the complex loading regimes through the test piece it is difficult to determine the extent of the pure shear region. Using F.E.A. Busfield (1997) developed an expression for the tearing in a pure shear test piece in terms of the force displacement data, with a correction to account for edge effects. This approach has been successfully implemented in previous works, Baumard *et al.*, (2013), and Asare and Busfield, (2011) and was again adopted here:

$$T = \frac{\int_0^x F \, dx}{t(L - c_X - (0.28h))} \qquad (16)$$

In this equation, the force, F, displacement, x, curve during loading is integrated to give the strain energy. This is divided by a function of the sample's thickness, t, total length, L, unstrained height, h, and the horizontal component of the crack length, c_x.

The fatigue tests were carried out at 0.5Hz at amplitudes ranging from 20% strain to 40% strain. A webcam was set up in front of the samples with a picture quality of 1240x 1024 pixels at 10 fps. Prior to testing a picture was taken of a ruler on the surface of the samples. This image quantified the number of pixels per mm in the pictures. Time-lapse photo logging software was then used to take pictures every 50 seconds, Figure 4. As the test frequency was 0.5Hz this equated to one picture every twenty five cycles.
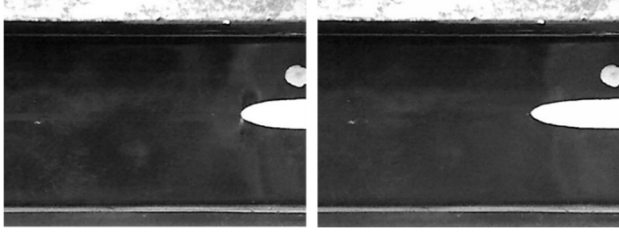
Figure 4: Crack tip image, N=0 and N=10000 cycles.

Once the data had been collected it was post-processed to determine the crack length at different cycles, the plot of which provided the crack growth rate. As shown in Figure 5, the crack growth rate is initially overstated, which is due to two spurious phenomena. Firstly the crack tip is unrealistically sharp and secondly the modulus is higher as only a limited amount of cyclic stress softening has taken place. By ignoring the early data a linear region, more characteristic of the material's steady state behaviour is observed, forms.
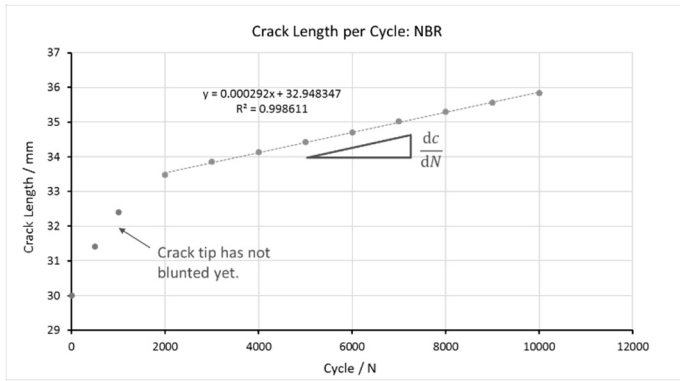

Figure 5: Variation in crack length with number of cycles.

The tearing energy was determined as an averaged value taken over several points in the linear region. Once the tearing energy and crack growth rate were determined the data was plotted to form fatigue profiles for both elastomers, Figure 6.
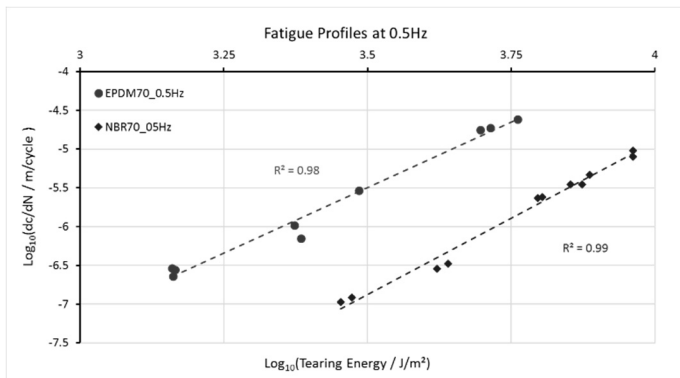

Figure 6: Fatigue profiles for the EPDM and NBR.

3.3 Static Crack Growth

In addition, the static crack growth behaviour was characterised. Due to viscoelastic relaxation the planar tension tear test geometry is not ideal for static tear tests. It was however important that the sample

was tested after being exposed to a similar load history to the samples cycled in pure shear.

To achieve this planar samples were first pre-cycled to 40% strain for 1,000 cycles at 0.5Hz. The test region was then cut into trouser tear specimens of 58x15x2mm, with the leg cut orientated to match the direction of flaws cut in to the original planar geometry. These were then characterised at tear rates from 0.05 mm/s to 0.0005 mm/s to form static tear profiles, shown in Figure 7. For trouser tear specimens:

$$T = \frac{2F\lambda}{h} - bw \qquad (17)$$

Here the tearing energy is given by the force, F, tearing the sample, the extension of the trouser legs, λ, and the resulting strain energy density, w, in them and the sample's thickness, h, and total width, b.
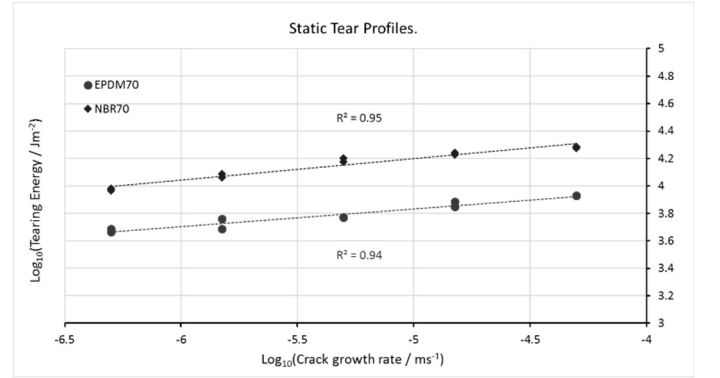

Figure 7: Static tear profiles for the EPDM and NBR.

3.4 Cyclic Stress Relaxation

Finally the cyclic stress relaxation behaviour was studied in this work. Viscoelastic relaxation in elastomers is split into two contributions, a physical contribution due to viscoelastic and filler effects, and a chemical contribution due to chemical degradation, Yamaguchi *et al.,* (2014). Over short time scales, the physical contribution dominates.

Cyclically loading under planar conditions was expected to induce some directionality to the polymer chains and filler degradation. This was likely to cause the relaxation to vary from cycle to cycle. To study this effect, planar samples were first pre-cycled for 1,000 cycles to 40% strain at 0.5Hz, removing stress softening effects.

They then underwent trapezoid loading cycles, in which the samples were strained to 40% at a rate equivalent to 0.5Hz before being held strained for 30 minutes, causing short term viscoelastic relaxation. They were then unloaded to complete the cycle. The data is shown in Figure 8.

As shown from the figures, an equilibrium profile is reached after only two cycles. The averaged relaxation data for each elastomer was used to characterise the tearing energy during the hold stage.
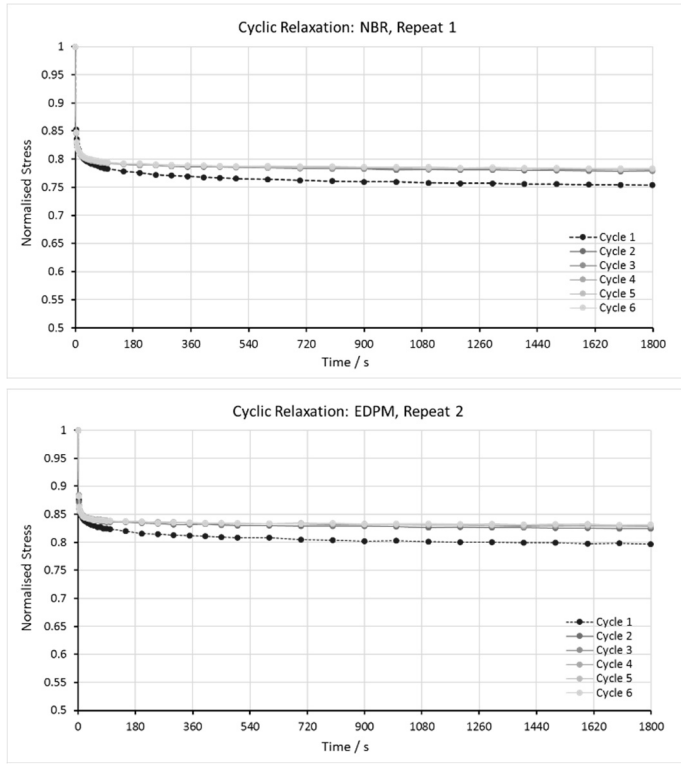
Figure 8: Cyclic relaxation of the NBR and EPDM.

3.5 Mixed Mode Fatigue

Mixed mode fatigue tests were run using planar tension crack growth test pieces. To further simplify the problem the samples were first pre-cycled for 1,000 cycles to 40% strain at 0.5 Hz, such that a steady state in the material's stress softening behaviour was reached. The tearing energy per cycle should therefore be relatively constant.

A 30mm flaw was cut into the specimens before they were put through a trapezoidal strain cycle. In the first second of the cycle the uncut section of the sample was loaded to 40% strain at a rate that was equivalent to loading at 0.5Hz. The sample was then held for 1797 seconds before being unloaded in one second followed by a one second hold stage. Each test consisted of 120, 30 minute cycles. Using a similar set up as for the cyclic tear tests, pictures were taken of the crack tip every 30 minutes to determine the crack growth rate, Figure 9. The results are shown in Tables 1 and 2.
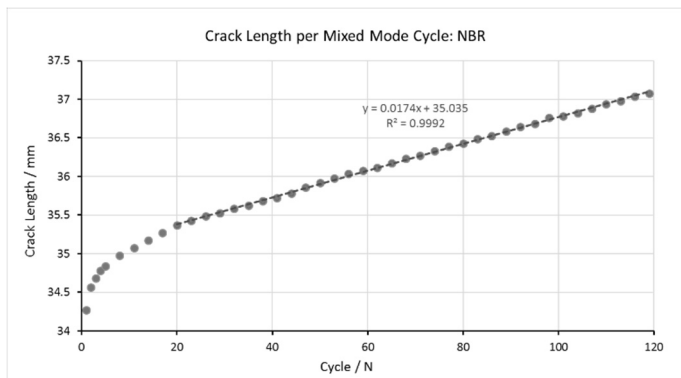

Figure 9: Variation in crack length with number of cycles.

4 RESULTS

The peak tearing energy was defined as the averaged value taken at every 10th cycle. Once this was known the cyclic component of the crack growth was readily determined from the fatigue profiles, Figure 6.

Finding the growth during the hold stage was a little more difficult. The tearing energy should decrease in line with relaxation, hence the tearing energy as a function of time was known. The static tear profiles relate the crack growth rate to the tearing energy. By combining these, one can plot the crack growth rate with time, Figure 10, the integral of which gives the crack growth during the hold stage.
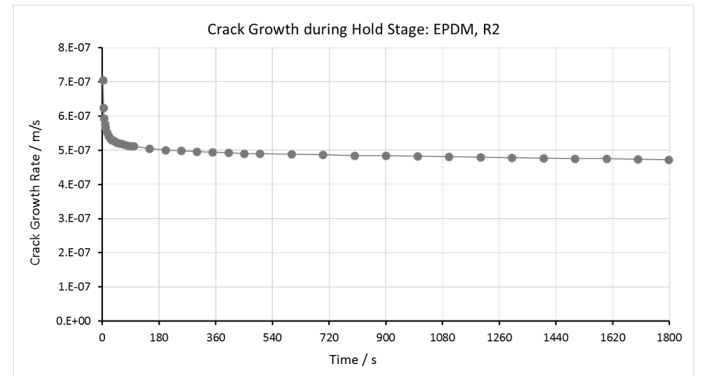

Figure 10: Crack growth during hold stage.

Table 1: Predication vs test data for mixed cycle, EPDM.

Variable	Source	EPDM, R1	EPDM, R2
T_{peak} /Jm^{-2}	Test	6091.8	5408.8
dC/dN Test /m·cycle^{-1}	Test	2.83E-04	2.36E-04
dc/dN Cycle /m·cycle^{-1}	Model	2.93E-05	1.96E-05
dc/dN Time /m·cycle^{-1}	Model	2.08E-03	8.76E-04
dC/dN Model /m·cycle^{-1}	Model	2.11E-03	8.95E-04
(dc/dN)$_{Model}$ / (dc/dN)$_{Test}$		7.44	3.80

Table 2: Predication vs test data for mixed cycle, NBR.

Variable	Source	NBR, R1	NBR, R2
T_{peak} /Jm^{-2}	Test	6884.6	7561.4
dC/dN Test /m·cycle^{-1}	Test	1.74E-05	3.27E-05
dc/dN Cycle /m·cycle^{-1}	Model	2.84E-06	4.11E-06
dc/dN Time /m·cycle^{-1}	Model	2.38E-05	4.23E-05
dC/dN Model /m·cycle^{-1}	Model	2.66E-05	4.65E-05
(dc/dN)$_{Model}$ / (dc/dN)$_{Test}$		1.53	1.42

5 DISCUSSION

Considering the complications of the model, for the predications to be within the correct order of magnitude for both elastomers is a good result. The NBR data in particular is a very good prediction all things considered. Slight variances between the two were expected due to a culmination of errors from the three characterisation methods. Furthermore, predications for very simple, single contribution, fatigue problems generally do not achieve perfect results either.

The cyclic crack growth contribution is likely to be over predicted as stress relaxation will cause the tearing energy during the unloading phase to be much lower, nevertheless the cyclic contribution appears to be minor. The main error arises in the calculation of the crack growth during the hold stage.

As the hold time is 1797 seconds, slight miscalculations in the static tear behaviour are amplified through the model. This is not helped by the logarithmic nature of the static tear plots which also magnifies small errors. Taking EPDM, R2 as an example, the correct predication requires the static tearing energy values to be 20% greater than the laboratory tests predicted. This demonstrates an impractical sensitivity to the static tear data which is notoriously difficult to characterise. The model provides a better predication for the NBR sample probably because the static term is less dominant and a better fit is achieved to for static tear data.

The NBR was more tear resistant than the EPDM, as shown in Figures 6 and 7. Analysing the mixed mode cycles this was benefitted by its relaxation behaviour. As the NBR relaxed further the tearing energy in it reduced faster, slowing the crack growth. This means that under fixed displacement tear conditions that viscoelastic relaxation actually enhances the component's fatigue life.

6 CONCLUSION

A mathematical model for predicting crack growth during mixed mode fatigue regimes was presented. The analytical model was compared against test data, and showed promising results, fitting within an order of magnitude for both elastomers tested. The difficulties encountered in matching the data was attributed to its sensitivity to errors in the static tear data. Of note, viscoelastic relaxation was shown to have a beneficial effect on the elastomer's fatigue resistance.

8 REFERENCES

Sakulkaew, K., Thomas, A.G., & Busfield, J.J.C., (2011). The effect of the rate of strain on tearing in rubber. *Polymer Testing*, *30*(2), 163–172.

Rivlin, R.S., & Thomas, A.G., (1953). Rupture of Rubber. I. Characteristic energy for tearing. *Journal of Polymer Science*, *10*(3), 291–318.

Griffith, A.A., (1921). The Phenomena of Rupture and Flow in Solids. *Philosophical Transactions of the Royal Society A: Mathematical, Physical and Engineering Sciences*, *221*, 163–198.

Kadir, A., & Thomas, A G., (1981). Tear Behaviour of Rubbers over a Wide Range of Rates. *Rubber Chemistry and Technology*, *54*(1), 15–23.

Fukahori, Y., Sakulkaew, K., & Busfield, J.J.C., (2013). Elastic-viscous transition in tear fracture of rubbers. *Polymer*, *54*(7), 1905–1915.

Busfield, J.J.C., Tsunoda, K., Davies, C.K.L., & Thomas, A.G., (2002). Contributions of time dependent and cyclic crack growth to the crack growth behavior of non strain-crystallizing elastomers. *Rubber Chem. Tech.*, *75*, 643–656.

Busfield, J. J. C., Ratsimba. C. H., Thomas. A. G., (1997). Crack growth and strain induced anisotropy in carbon black filled natural rubber. *Journal of Natural Rubber Research*, 12, 131-141.

Baumard, T.L.M., Thomas, A.G., & Busfield, J.J.C., (2013). Evaluation of the tearing energy in a radial tyre. In Alonso (Ed.), *Constitutive Models for Rubber VIII*. San Sebastian: CRC Press.

Asare, S., & Busfield, J.J.C., (2011). Fatigue life prediction of bonded rubber components at elevated temperature. *Plastics, Rubber and Composites*, *40*(4), 194–200.

Yamaguchi, K., Thomas, A.G., & Busfield, J.J.C., (2015). Stress relaxation, creep and set recovery of elastomers. *International Journal of Non-Linear Mechanics*, *68*, 66–70.